SPECIAL TOPICS— Acoustics

Nonlinear response of ultrasound contrast agent microbubbles: From fundamentals to applications*

Xu-Dong Teng(滕旭东), Xia-Sheng Guo(郭霞生)†, Juan Tu(屠娟), and Dong Zhang(章东)‡

Institute of Acoustics, Key Laboratory of Modern Acoustics (MOE), School of Physics, Nanjing University, Nanjing 210093, *China*

(Received 11 May 2016; revised manuscript received 10 July 2016; published online 25 October 2016)

Modelling and biomedical applications of ultrasound contrast agent (UCA) microbubbles have attracted a great deal of attention. In this review, we summarize a series of researches done in our group, including (i) the development of an all-in-one solution of characterizing coated bubble parameters based on the light scattering technique and flow cytometry; (ii) a novel bubble dynamic model that takes into consideration both nonlinear shell elasticity and viscosity to eliminate the dependences of bubble shell parameters on bubble size; (iii) the evaluation of UCA inertial cavitation threshold and its relationship with shell parameters; and (iv) the investigations of transfection efficiency and the reduction of cytotoxicity in gene delivery facilitated by UCAs excited by ultrasound exposures.

Keywords: ultrasound contrast agents, microbubbles, nonlinear response, inertial cavitation, DNA transfection

PACS: 43.25.+y, 43.80.+p **DOI:** 10.1088/1674-1056/25/12/124308

1. Introduction

It is more than three decades since micron sized bubbles were utilized in clinic as ultrasound contrast agents (UCAs). UCA microbubbles are usually insoluble gas cores (e.g., perfluorocarbon, sulfur hexafluoride) encapsulated by thin coatings (e.g., lipid, albumin, and polymer) that help to prevent the bubbles from dissolving into water. Taking advantages from the compressible gas cores and resonance-induced intense scattering,[1] UCAs are initially injected into the bloodstream and utilized to enhance the acoustic contrast ratio of diagnostic ultrasound (US) images related to specific cardiographic or radiologic features.[2] However, recently increasing interest has been aroused in some novel diagnostic as well as therapeutic applications of UCAs (e.g., targeted molecule imaging, thrombolysis, gene delivery/drug delivery, tumor treatment and hemostasis),[3–10] most of which benefit from the microbubble nonlinear behaviors, such as the generations of harmonics and ultrasound-induced cavitation activities.

Most commercialized UCAs that have been approved for clinical use are encapsulated by lipid or albumin shells. Compared with stiffer coating materials (e.g., polymer), the flexible soft coatings enable UCA bubbles to sustain large amplitude oscillations. However, it was initially assumed that UCA microbubbles underwent linear oscillations only when being sonicated at the frequencies of biomedical ultrasound, while the nonlinear responses of UCAs received insufficient attention until the mid-nineties.[11] After that, several pioneering formulated bubble models were developed[12–15] based on approximations and scaling arguments from the well-known Rayleigh-Plesset (RP) equation.[16,17] By taking into consideration the viscoelasticity and strain-stress relationship of thin shell materials, the Kelvin–Voigt constitution law and Hooke's law were used to describe more complicated nonlinear responses (e.g., compression-only behavior) of UCA microbubbles. These semi-empirical models have achieved a lot of success in simulating the dynamic behaviors of albumin-shelled Albunex®microbubbles.[15,18,19] Lipid-shelled microbubbles, benefiting from their thinner shells (albumin: $\sim$ 15 nm, lipid: 2 nm$\sim$4 nm)[15,20,21] and higher flexibilities, have been more broadly used in recent years and effectively propelled the development of new bubble models. In these models, the radiation damping,[22] Newtonian interfacial rheological properties[23,24] or Maxwell constitution law might take the place of the Kelvin–Voigt constitution law to describe viscoelastic characteristics of the thin lipid shell.[25]

In addition to numerical modeling work, some new experimental techniques were also adopted in exploring the physical natures of UCAs. With the help of high-speed imaging,[22] the uncommon behaviors of microbubbles such as "compression-only",[26–31] "thresholding",[32,33] and "shear-thinning"[34–38] were unprecedentedly found, which could lead to extraordinary nonlinear responses of UCAs and prompted further mod-

*Projects supported by the National Natural Science Foundation of China (Grant Nos. 81127901, 81227004, 11374155, 11274170, 11274176, 11474001, 11474161, 11474166, and 11674173), the National High-Technology Research and Development Program, China (Grant No. 2012AA022702), and Qing Lan Project of Jiangsu Province, China.

†Corresponding author. E-mail: guoxs@nju.edu.cn

‡Corresponding author. E-mail: dzhang@nju.edu.cn

© 2016 Chinese Physical Society and IOP Publishing Ltd

ification and improvement of more sophisticated bubble models. In a representative work done by Marmottant *et al.*,[39] based on which the "compression-only" and "thresholding" behaviors of UCAs could be effectively simulated, the surface tension of the bubble shell was partially characterized by an empirical radius threshold below which the bubble might buckle and a critical tension value at which the shell might break up. It was also proposed by Doinikov *et al.* that the "shear-thinning" phenomenon could be accounted for by describing the viscous stress in the shell as a function of the shear rate.[40] However, the above modeling efforts were always subjected to the dependences of the shell viscoelastic parameters on the initial bubble radius, which was believed to conflict with the general physics of natural materials.[21] Therefore, it was suggested that a more comprehensive model should be taken to describe the complex theological nature of UCA microbubbles by taking into account the nonlinear changes in both shell elasticity and viscosity.[40]

Although there seems to be a lot of debate about the shell properties of UCA microbubbles, it is all actually related to the constant or variable elastic and viscous parameters of the shell materials. Generally, shell parameters could be estimated by fitting measured acoustic response data to coated bubble models under a prior knowledge of the size distribution and concentration of the bubble solution. Existing techniques to measure acoustic responses include bulk measurements of microbubble attenuation/scattering spectra,[41,42] optical microscopy,[22,38,43] flow cytometry,[21,44] and light scattering.[21,45] But none of the above techniques can provide an all-in-one system for characterizing the physical properties of UCAs, despite the fact that there is an urgent need to perform all the measurements quickly and easily.[21]

In the applications of UCAs, one of the most important mechanisms involved in US-induced non-thermal bioeffects is cavitation.[42] There are two types of acoustic cavitations: "inertial" (or transient) and "non-inertial" (or stable). The Inertial cavitation (IC) refers to the phenomenon that under a sufficiently high acoustic pressure amplitude (above a threshold level), the microbubbles would first grow in volume and then implode violently.[46] On the contrary, the process that bubbles are forced to experience small-to-moderate oscillations is regarded as non-inertial cavitation. It is essential to take control of IC activities in different diagnostic/therapeutic applications, since excessive IC energy could cause some unfavorable side-effects, such as vascular endothelial damage,[47] hemorrhage due to capillary rupture,[48] cell apoptosis,[49,50] and DNA fragmentation.[51] The introduction of UCAs could significantly lower the IC thresholds by providing additional gas bubbles to serve as cavitation nuclei. Compared with that of free gas bubbles, the IC threshold of encapsulated UCA bubbles could be more dependent on their shell material which is believed to increase the mechanical stiffness as well as the acoustic energy absorption. Flynn *et al*. predicted that a critical maximum radius of an oscillating bubble must reach twice the equilibrium radius (R_0) before it undergoes IC collapse.[52] However, it would be much easier to quantify the IC-induced broadband noise signals than to monitor the transient bubble oscillations in most applications.[42]

One important issue that is related to the nonlinear responses of UCA microbubbles (especially the cavitation activities), should be the bubble-cell interactions induced by ultrasound (US) exposures,[46] which has aroused broad interest in the physics and medicine communities. With microbubbles oscillating in violent (inertial cavitation) or non-violent (non-violent cavitation) regimes, there could emerge short-lived pores on the cell membrane.[50,53,54] This process is called "sonoporation", which can enhance the permeabilization of the cell membrane and, in turn, allow for the transfer of genes or drugs between the intra- and extra-cellular medium.[53,55] The possible mechanism of sonoporation could contribute to the IC-induced "jetting" behavior which might penetrate the cell membrane, the acoustic microstreaming localized around oscillating bubbles, or shear stress caused by the bubble expansion that could transiently open up the cell membrane.[53] There have been some successes in microbubble mediated gene/drug delivery both *in vitro* and *in vivo*, such as delivering pDNA encoding luciferase in the left ventricle of anesthetized rats,[56] in strengthening the bone formation in the hind limb muscle of mice which provides a promise for sonoporation aided bone induction,[57] and also in intro-tumoral injection of anti-tumor genes followed by percutaneous sonication in cancer therapy.[53,58–61] Although sonoporation is believed to be promising for developing the gene therapy and targeted drug delivery, this technique is still challenged by cell targeting, sonoporation efficiency, microbubble lifetime, different bio-signals activated in different or even the same cell lines, the lack of homogeneity in sonoporation setups as well as the adopted acoustic parameters. However, what is more important is that a consensus of the exact mechanism linking microbubble dynamic behaviors and the sonoporation outcomes is still lacking.

Therefore, the major problems about UCA microbubbles that are confronted nowadays, which are also hot issues in the area of biomedical ultrasound, should include at least four respects, i.e., (i) characterizations of the UCAs parameters in an accurate and reliable way; (ii) new formulations which could describe various experimentally-observed nonlinear behaviors of UCAs; (iii) exploration of new biomedical-applications of UCAs; and (iv) in-depth understanding of physical mechanisms involved in new biomedical observations.

Summarized in this review is a series of our researches regarding the nonlinear responses of microbubbles, ranging

from the fundamental formulations to recent work about DNA delivery mediated by UCA microbubbles. The obtained results are also compared with those published literature data.

2. Bubble characterization

Motivated by the importance of the shell for microbubble stability and volumetric response to acoustic incidence, and also for molecular targeting and therapy, the technique of light scattering was combined with a commercial flow cytometer to perform an all-in-one characterization of the physical properties of Definity®(Lantheus Medical Imaging, North Billerica, MA) and SonoVue®(Bracco Diagnostics Inc., Geneva, Switzerland) microbubbles.[21,44,45] A diagram of the experimental setup is given in Fig. 1. The incident laser beam was scattered by microbubbles in the flow channel, and the scattered lights were collected and focused onto a field stop. Diverging from the field stop, the light was then split with a $\sim 6\%$ glass coverslip splitter and collected with side-scatter PMT detectors. The flow channel was modified by bonding a small PZT transducer to the side of a custom-built quartz flow cell with a 150-μm flow channel. Hence, any instantaneous change in bubble size could be characterized through the variation in the intensity of the scattered light, and the output voltage of the flow cytometer could be converted into a radius according to the Mie scattering theory[62,63] and a specified calibration routine.[21,45]

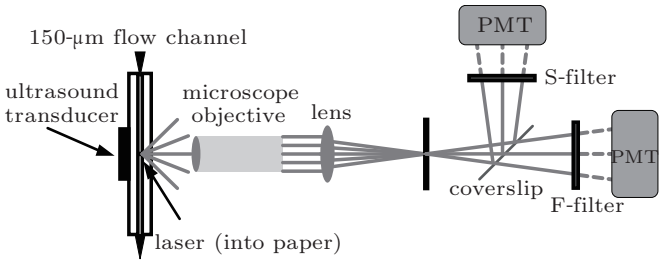


Fig. 1. Diagram of the experimental setup. Reproduced from Ref. [21].

It should be considered that the output measurement which is reproduced in Fig. 2 actually contained two parts: (a) a low-frequency part corresponding to the equilibrium radius of each individual particle, and (b) a high-frequency signal contributed by the oscillation of the bubble when ultrasound was turned on. Therefore, by utilizing a low-pass and high-pass filter respectively, the size distribution and bubble concentration of the UCAs could be identified from part (a), while the shell parameters could be estimated by fitting the radius-time curves obtained from part (b) with an appropriate numerical model, such as the Marmottant formulation.[39] Another advantage of this all-in-one solution was to generate thousands of data sets at different pressure levels, which made it possible to easily verify the validities of different bubble models.

It was found in the studies that the shell viscosity increased with increasing R_0, which was consistent with the experimental observations in Refs. [22], [38], [40], [43], and [45]. However, the elastic modulus nearly remained constant throughout the measurements, while Doinikov *et al.*[40] predicted that the shell elasticity should obey the rule: "strain softening" increasing with the augment of R_0. This disparity has also become the impetus to further improve the bubble model which could account for the complex rheological natures of both the shell elasticity and viscosity. In the work by Paul *et al.*, it was found that a quadratic or exponential elasticity model could better explain the low subharmonic threshold than the Marmottant model.[62] Tsiglifis *et al.* defined a strain softening Mooney–Rivlin or a strain-hardening Skalak law, which made the shell elasticity to vary with bubble deformation.[63] But Doinikov *et al.* argued that the dependence of shell elasticity on bubble radius could be an artifact since it conflicted with the fundamental physics of materials.[40] Therefore, confusions still exist in the modeling work targeting at microbubble nonlinear responses.

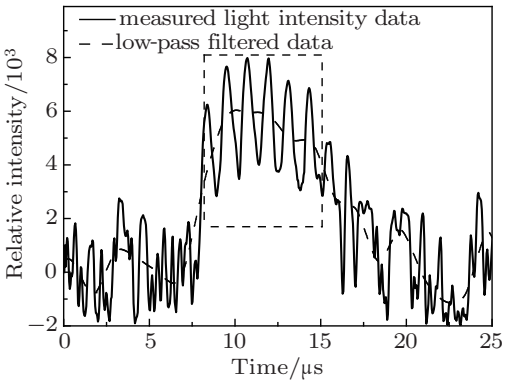


Fig. 2. Measured light intensity scattered from a definity microbubble driven by a 1-MHz ultrasound pulse. The signal within the rectangle could be high-pass filtered and converted into a radius-time curve. Reproduced from Ref. [21].

3. Modelling the shell nonlinearity

As mentioned above, there have been suggestions that the dependences of shell viscosity and elasticity on the equilibrium R_0 should result from two types of rheological behaviors known as "shear-thinning"[22,38,40,45] and "strain-softening",[40,45] respectively. Thus, a new bubble model has been developed by our group, in which both nonlinear shell elasticity and viscosity were taken into account by applying a nonlinear rheological law to the shell viscos term in the Marmottant model.[64] The new model was validated by fitting experimentally measured radius-time curves, and was demonstrated to be able to reproduce the "compression-only" behavior while reducing the dependences of shell parameters on R_0.

In the well-known Church model,[15,19] the encapsulating effect of the bubble shell was described with the adoption of the Kelvin–Voigt constitutive law. By assuming the thin-shell limit, the shell term in the Church model could be simplified

into

$$S = S_{\text{elasticity}} + S_{\text{viscosity}} = 4\chi \frac{R_e}{R}\left(\frac{1}{R_e} - \frac{1}{R}\right) + 4\kappa_s \frac{\dot{R}}{R^2}, \quad (1)$$

in which R and $\dot{R}$ represent the instantaneous bubble radius and its time derivative, respectively; R_e is the equilibrium radius of the microbubble; χ and κ_s are the shell elasticity modulus and viscosity, respectively. Since this model regards χ and κ_s as constants, it is more appropriate to describe small-amplitude oscillations of bubbles and challenged by simulating the bubbles' nonlinear responses such as the "compression-only" behavior. Considering that the surface area per phospholipid molecule varied during the oscillation of a phospholipid coated bubble, Marmottant *et al.* regarded the bubble shell as a two-dimensional viscoelastic medium. By taking into account the shell buckling and rupture, they described the radius-dependent surface tension $\sigma(R)$ in three different regimes as follows:

$$\sigma(R) = \begin{cases} 0, & R \le R_{\text{buckling}} \approx R_0, \\ \chi\left(\frac{R^2}{R_{\text{buckling}}^2} - 1\right), & R_{\text{buckling}} < R \le R_{\text{breakup}}, \\ \sigma_{\text{water}} = 0.072\ \text{N}\cdot\text{m}^{-1}, & R > R_{\text{breakup}}, \end{cases} \quad (2)$$

where R_{buckling} is the lower limit of the bubble radius, below which the shell undergoes buckling; above R_{breakup} the bubble turns ruptured and the surface tension becomes that of the gas-liquid interface. In this case, the shell encapsulation effect could be described as

$$S = S_{\text{elasticity}} + S_{\text{viscosity}} = \frac{2\sigma(R)}{R} + 4\kappa_s \frac{\dot{R}}{R^2}, \quad (3)$$

whose linearization based on the thin-shell assumption and small-amplitude oscillation leads to a description identical to the shell elastic part in the Church model.[38]

Since the Marmottant model still leads to an R_0-dependent viscosity, a more general nonlinear model was proposed by our group. The shell viscosity was considered as a function of the shell's shear rate $(\dot{R}/R)$ instead of a constant, while the Cross law was adopted to model the rheological behavior of the shell material. The nonlinear shell viscous was modified as

$$4\kappa\left(\frac{\dot{R}}{R}\right)\frac{\dot{R}}{R^2} = \frac{4\kappa_0}{1+\alpha|\dot{R}|/R}\frac{\dot{R}}{R^2}, \quad (4)$$

where κ_0 was the shell viscous parameter and α was a characteristic time constant. The eventual bubble dynamics model has the following form:

$$\rho_l\left(R\ddot{R} + \frac{3}{2}\dot{R}^2\right) = \left[P_0 + \frac{2\sigma(R_0)}{R_0}\right]\left(\frac{R_0}{R}\right)^{3\gamma}\left(1 - \frac{3\gamma}{c}\dot{R}\right) - \frac{2\sigma(R)}{R} - 4\eta_l\frac{\dot{R}}{R} - 4\kappa\left(\frac{\dot{R}}{R}\right)\frac{\dot{R}}{R^2} - P_0 - P_{\text{ac}}(t), \quad (5)$$

which is also referred to as the "nonlinear elasticity and viscosity" (NSEV) model. In Eq. (5), ρ_l and η_l are the density and viscosity of a Newtonian liquid, P_0 is the ambient pressure, γ is the polytropic exponent of the gas, and $P_{\text{ac}}(t)$ is the sinusoidal incident acoustic pressure.[65]

The NSEV model was validated by fitting the measured radius-time curves and comparing with two existing models. In Fig. 3(a), the newly proposed model is compared with the Doinikov model by examining their fittings to experimentally observed dynamic responses of a phospholipid-coated, perfluorocarbon microbubble measured with high-speed optical imaging. One can also see from the comparison that the proposed NSEV model provides better fitting to the experimental result that demonstrates obvious "compression-only" behavior. Another comparison given in Fig. 3(b) is carried out between the NSEV and Marmottant models, in which both models are fitted to a radius-time curve of a SonoVue microbubble measured using the light scattering technique. From the illustration and the minimum root mean square error (RMSE) it is suggested that by using the Cross law to modify the shell viscous term, the NSEV model could perform better when simulating the nonlinear responses of lipid-coated SonoVue microbubbles.

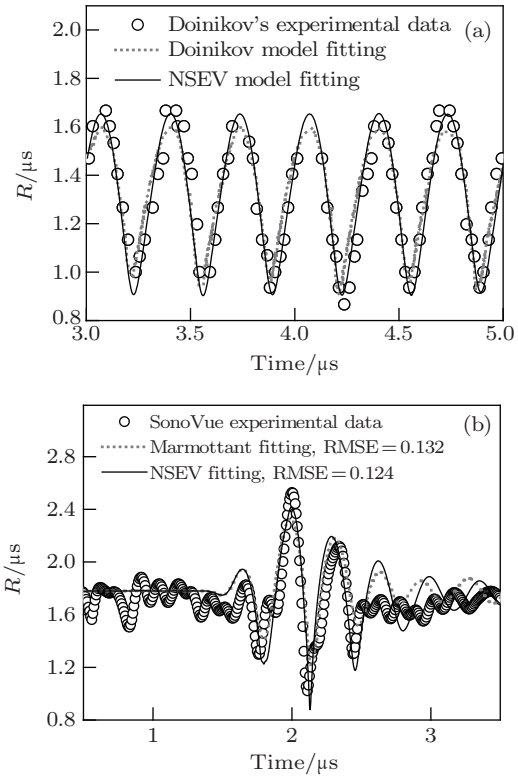


Fig. 3. Validations of the proposed NSEV model by (a) fitting the bubble dynamic responses acquired with a high-speed optical imaging system, and by (b) fitting the radius-time curve of a SonoVue microbubble measured with light scattering technology. Reproduced from Ref. [65].

The main objective of developing the NSEV model was to solve the problem that most previous bubble models assume R_0-dependences of shell parameters. Thus, the shell elasticity and viscosity parameters were also estimated by fitting measured radius-time curves with the NSEV model, and the fitting results were compared with those obtained from linearized and full Marmottant models. Figure 4 shows that the linearized and full Marmottant models predict that the shell parameters (at least the shell viscosity) increase with the augment of R_0 from the NSEV model, but both of the parameters remained nearly constant. One limitation of the NSEV model lies in the increased number of parameters, which, as pointed out by Faez *et al*., has a drawback that the merit of the applied material law and the resulting parameterization cannot be judged easily.[11]

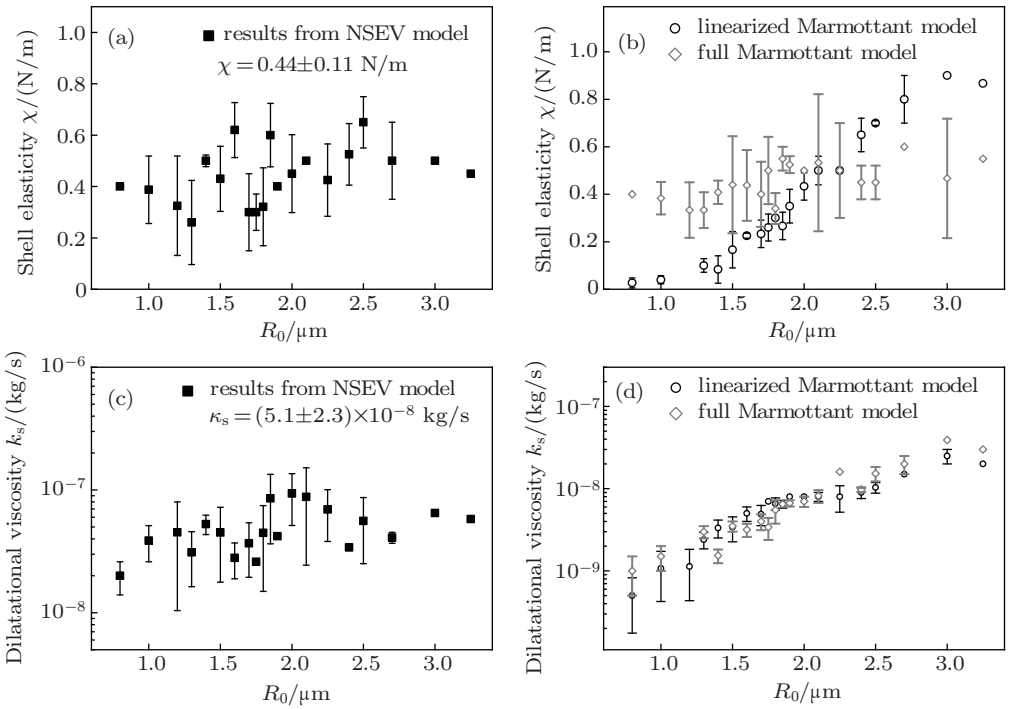


Fig. 4. Shell parameters of SonoVue bubbles: elastic modulus estimated by using (a) the NSEV model, (b) the linearized and full Marmottant models, (c) the NSEV model for estimating the viscosity parameter, and (d) the linearized and full Marmottant models. Reproduced from Ref. [11].

4. Detection of IC threshold

When the acoustic pressure of incident wave is greater than a typical threshold, IC behaviors will emerge in the dynamic responses of UCA microbubbles. Typically, a passive cavitation detection (PCD) system could be utilized to detect the emission signals of IC microbubbles, which could be characterized by a sudden enhanced frequency spectra caused by the broadband noise generated from bubble destructions.[64,66] The so-called IC threshold could be determined by quantifying the IC "dose" (ICD), which evaluates the "amount" of IC energy accumulated during a certain sonication period.[64] In brief, PCD-detected waveforms in time domain were first transformed into frequency spectra; within a specific frequency window between two neighborhood harmonics, a root mean square (RMS) amplitude of the broadband noise was determined for each measurement; the ICD could then be evaluated by integrating the RMS amplitudes as a function of time over the exposure "on" time period.[42,64,67] For each specified sample, the ICD data as a function of calibrated acoustic peak negative pressure P- were compared by using Student's t-test. The IC threshold was eventually defined as the P-level at which the ICD is statistically increased from the baseline, while a p-value smaller than 0.05 is usually accepted as a significant value.

In a previous study, the IC thresholds of two types of commercial UCA microbubbles were characterized, while their dependences on acoustic parameters as well as shell properties were also investigated.[42] One of them was lipid-shelled SonoVue, the other was albumin-shelled KangRun®(RunKun Pharmaceutical Co., Hunan, China) microbubbles. Acoustic scattering measurements were carried out to evaluate microbubble IC activity.[42] Meanwhile, the shell parameters of microbubbles were determined by fitting Sarkar's bubble dynamic model to the obtained attenuation spectrum, while the size distributions of microbubbles were measured with the help of a particle size analyzer.

The results shown in Fig. 5 illustrated the IC thresholds of both SonoVue and KangRun microbubbles decrease with UCA volume concentration increasing, which were also demonstrated by other researchers.[68–71] On the other hand, the IC threshold appears to be a decreasing function of acous-

tic pulse length, although it tends to reach a "saturation" level as the pulse length is longer than 20 cycles. It could be explained by the fact that it took a few cycles for the source transducer to "ring up" to the steady state. Therefore for short pulses (e.g., five cycles), the actual acoustic energy that was supplied to each microbubble was smaller than that of the long pulse case (e.g., more than 20 cycles). As the pulse length went longer, the IC thresholds would be less affected by the "ring up" issue. As far as the physical properties of the shell materials were concerned, the albumin-shelled KangRun bubbles had relatively larger elasticity and viscosity than lipid-shelled SonoVue, while the latter had a lower IC threshold in all the involved cases. It was hypothesized that the damping caused by larger elastic and viscous parameters might play an adverse role in facilitating the IC activities.

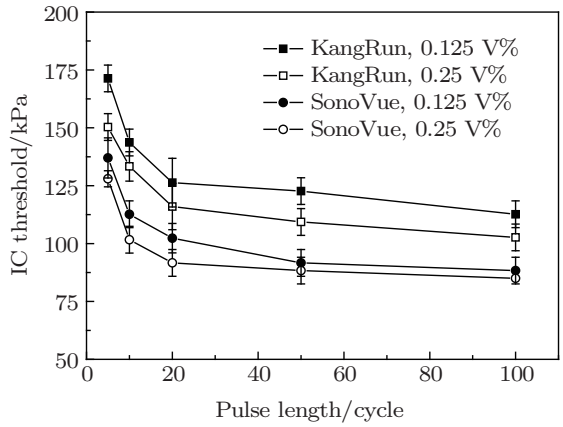


Fig. 5. Variations of IC threshold with pulse length measured for lipid-coated SonoVue and albumin-coated KangRun microbubbles at different volume concentrations. Reproduced from Ref. [42].

5. Cavitation involved DNA transfection

The studies show that the US-mediated microbubble destruction can enhance the DNA transfection efficiency by up to several orders of magnitude both *in vitro* and *in vivo*.[7,70–72] Although the exact mechanism involved in the ultrasonic sonoporation process has not been fully understood, there has been a hypothesis that US-induced IC activities should play an important role.[46,55,73] It was suggested that UCA microbubbles which collapsed in the IC process could lead to high shear stress which might generate the transient pores at the cell membrane.[68,69,74] During the previous studies in our group, different cell lines were investigated to study how the IC activity affected US-mediated DNA transfection.

In a series of experiments,[74] 1-MHz US pulses were exposed to the solution of MCF-7 cells (human breast cancer cells) mixed with polyethylenimine (PEI): DNA complex and UCA microbubbles; the ICDs were quantified using a PCD system; a flow cytometry was utilized to evaluate the DNA transfection efficiency; PI dying followed by flow cytometry was adopted for cell viability examination; the sonopores were observed with the help of scan electron microscopy (SEM). The results reproduced in Fig. 6 show that with the enhancement of ICD, the measured DNA transfection efficiency initially increases linearly to about 50% then tends to saturate (Fig. 6(a)), while the pore size continues to be enlarged (Fig. 6(c)); on the contrary, the cell viability decreases linearly (Fig. 6(b)), which leads to a self-evident result that there exists a negative correlation between the cell viability and the pore size (Fig. 6(d)).

Another important issue involved in US-mediated DNA transfection should be the cytotoxicity of IC activities, or whether it is possible to improve the transfection efficiency without lowering the cell viability, which is highly concerned especially in clinical applications. To make a clarification, experiments were carried out with branched polyethylenimine (bPEI)-mediated DNA (an isoform of the vascular endothelial growth factor, $VEGF_{165}$) transfection of HEK 293T cells in which ultrasound sonicated microbubbles were also involved.[75] The enhancement of transfection efficiency that was contributed from the IC microbubbles was surprisingly not observed. It was also found that when only the cytotoxicity of bPEI was taken into account (i.e., ICD = 0, US sham), cell viability significantly decreased with increasing PEI nitrogen: the DNA phosphate (N/P) ratio, and at N/P = 7 the cell viability reached its minimum of $\sim 55\%$. But if the bPEI was absent, even though the ICD reached its highest level, the cell viability was only lowered to $\sim 80\%$. Hence, the IC activity itself showed less cytotoxicity than bPEI. It was also indicated that there were synergistic deleterious effects of microbubble IC activity and bPEI on cell viability,[76] which reduced to $\sim 20\%$ when IC and bPEI both played their parts. However, when the N/P ratio was adjusted to 4, only $\sim 40\%$ cell apoptosis was observed while the transfection efficiency remained high. Therefore, a parameter optimization was usually required in these experiments.

Although the results in Fig. 6 provide a solid proof to the importance of IC activities for the US-mediated DNA transfection, it was also argued that shear stress resulting from microstreaming in the neighborhood of moderately pulsating bubbles could also be responsible for sonoporation.[76,77] In the experiments, it was also found that the shear stress monotonically increased with the rise of acoustic peak negative pressure.[78] As indicated by Tran *et al.*, sonicated bubbles could have activated the electrophysiologic cell activities by their "cellular massage" action, which actually corresponded to the moderate shear stress generated by nearby oscillating bubbles.[79] Therefore, the enhanced DNA transfection efficiency observed in the experiments might take the advantages from two categories: the shear stress generated by the microstreaming in the nearby oscillating microbubbles, and the

violent non-linear oscillating IC bubbles that could lead to the significant cell deformation or sonoporation. However, since the transfection efficiency was found to be relatively low in the weak IC case as indicated in Fig. 6(a), it is believed here that IC-related sonoporation could be the dominant role in enhancing ultrasound involved DNA transfections.

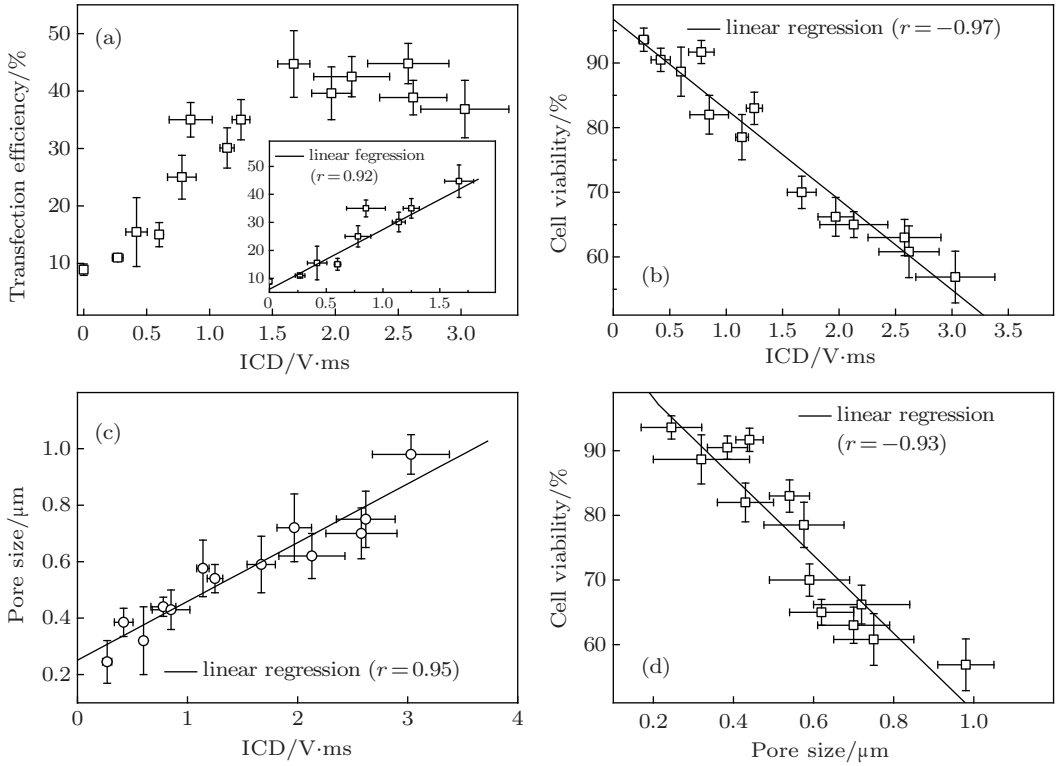


Fig. 6. (a) The DNA transfection efficiency versus ICD; (b) the cell viability versus ICD; (c) the sonopore size versus ICD; (d) the cell viability versus sonopore size. Reproduced from Ref. [74].

6. Conclusions

Increasing research interest focuses on nonlinear responses of UCA microbubbles, and some important features regarding this topic are discussed in the current review paper. It is found that by using an all-in-one characterization system, the shell parameters of UCA can be evaluated quickly and easily. Furthermore, the dependence of shell viscosity on the equilibrium bubble radius, which is believed to be an artifact resulting from the simplification of bubble models, is worked out by applying the Cross law to the Marmottant model so that nonlinear rheological properties of UCA shell material can be well described. The new model involves neither of R_0-dependences for both elasticity and viscosity of the bubble shell. More efforts are also made to measure the inertial cavitation thresholds of UCAs, and the results suggest that the damping caused by larger shell elasticity and viscosity might play an adverse role in promoting the IC activities. The quantification method of evaluating the energy of IC activity is then used to identify whether it is correlated to the enhancement of DNA transfection efficiency mediated by sonicated microbubbles; it is concluded that the IC-facilitated sonoporation could play a dominant role in enhancing UCA-mediated DNA transfection, while the cytotoxicity of ultrasound-induced IC activity is controllable with optimized acoustic driving parameters.

References

[1] Pace N G, Cowley A and Campbell A M 1997 *J. Acoust. Soc. Am.* **102** 1474
[2] Goldberg B B, Raichlen J S and Forsberg F 2001 *Ultrasound contrast agents: basic principles and clinical applications*, 2nd edn. (London: Martin Dunitz)
[3] Hu J W, Qian S Y, Sun J N, Lu Y B and Hu P 2015 *Chin. Phys. B* **24** 094301
[4] Cao H, Huang W J, Qiao J H, Wang Y P and Zhao H J 2015 *Chin. Phys. Lett.* **32** 034301
[5] Stride E P and Coussios C C 2010 *P. I. Mech. Eng. H* **224** 171
[6] Wang L, Tu J, Guo X S, Xu D and Zhang D 2014 *Chin. Phys. B* **23** 124302
[7] Ferrara K, Pollard R and Borden M 2007 *Ann. Rev. Biomed. Eng.* **9** 415
[8] Kennedy J E 2005 *Nat. Rev. Cancer* **5** 321
[9] Everbach E C and Francis C W 2000 *Ultrasound Med. Biol.* **26** 1153
[10] Escoffre J M, Mannaris C, Geers B, Novell A, Lentacker I, Averkiou M and Bouakaz A 2013 *IEEE Trans. Ultrason. Ferrelec. Freq. Control* **60** 78
[11] Faez T, Emmer M, Kooiman K, Versluis M, van der Steen A and de Jong N 2013 *IEEE Trans. Ultrason. Ferrelec. Freq. Control* **60** 7
[12] Dejong N and Hoff L 1993 *Ultrasonics* **31** 175
[13] Dejong N, Cornet R and Lancee C T 1994 *Ultrasonics* **32** 455
[14] Dejong N, Cornet R and Lancee C T 1994 *Ultrasonics* **32** 447
[15] Church C C 1995 *J. Acoust. Soc. Am.* **97** 1510
[16] Rayleigh 1917 *Philos. Mag.* **34** 94
[17] Plesset M S 1949 *J. Appl. Mech.-T. Asme* **16** 277
[18] Roy R A, Madanshetty S I and Apfel R E 1990 *J. Acoust. Soc. Am.* **87** 2451
[19] Hoff L, Sontum P C and Hovem J M 2000 *J. Acoust. Soc. Am.* **107** 2272
[20] Chomas J E, Dayton P, Allen J, Morgan K and Ferrara K W 2001 *IEEE Trans. Ultrason. Ferrelec. Freq. Control* **48** 232
[21] Tu J, Swalwell J E, Giraud D, Cui W C, Chen W Z and Matula T J 2011 *IEEE Trans. Ultrason. Ferrelec. Freq. Control* **58** 955

[22] Morgan K E, Allen J S, Dayton P A, Chomas J E, Klibanov A L and Ferrara K W 2000 *IEEE Trans. Ultrason. Ferrelec. Freq. Control* **47** 1494

[23] Chatterjee D and Sarkar K 2003 *Ultrasound Med. Biol.* **29** 1749

[24] Sarkar K, Shi W T, Chatterjee D and Forsberg F 2005 *J. Acoust. Soc. Am.* **118** 539

[25] Doinikov A A and Dayton P A 2007 *J. Acoust. Soc. Am.* **121** 3331

[26] Sijl J, Dollet B, Overvelde M, Garbin V, Rozendal T, de Jong N, Lohse D and Versluis M 2010 *J. Acoust. Soc. Am.* **128** 3239

[27] Emmer M, Van Wamel A, Goertz D E and De Jong N 2007 *Ultrasound Med. Biol.* **33** 941

[28] Viti J, Mori R, Guidi F, Versluis M, de Jong N and Tortoli P 2012 *IEEE Trans. Ultrason. Ferrelec. Freq. Control* **59** 2818

[29] van der Meer S M, Marmottant P G, Hilgenfeldt S, Versluis M, Lohse D, Chin C T, Bouakaz A, Mastik F, Emmer M and de Jong N 2005 *IEEE Ultrasonics Symposium*, Vols. 1–4, pp. 974–976

[30] De Jong N, Emmer M, Chin C T, Bouakaz A, Mastik F, Lohse D and Versluis M 2007 *Ultrasound Med. Biol.* **33** 653

[31] Sijl J, Overvelde M, Dollet B, Garbin V, de Jong N, Lohse D and Versluis M 2011 *J. Acoust. Soc. Am.* **129** 1729

[32] Emmer M, van Wamel A, Goertz D E, Versluis M and de Jong N 2006 *Proc. IEEE Ultrason. Symp.*, Vols. 1–5, pp. 1545–1547

[33] Overvelde M, Garbin V, Sijl J, Dollet B, de Jong N, Lohse D and Versluis M 2010 *Ultrasound Med. Biol.* **36** 2080

[34] Hay T A, Ilinskii Y A, Zabolotskaya E A and Hamilton M F 2013 *J. Acoust. Soc. Am.* **134** 1454

[35] Shams M M, Dong M Z and Mahinpey N 2014 *Aiche J.* **60** 2660

[36] Shen Y Y, Longo M L and Powell R L 2008 *J. Colloid Interf. Sci.* **327** 204

[37] Faez T, Emmer M, Docter M, Sijl J, Versluis M and de Jong N 2011 *Ultrasound Med. Biol.* **37** 958

[38] van der Meer S M, Dollet B, Voormolen M M, Chin C T, Bouakaz A, de Jong N, Versluis M and LohseD 2007 *J. Acoust. Soc. Am.* **121** 648

[39] Marmottant P, van der Meer S, Emmer M, Versluis M, de Jong N, Hilgenfeldt S and Lohse D 2005 *J. Acoust. Soc. Am.* **118** 3499

[40] Doinikov A A, Haac J F and Dayton P A 2009 *Ultrasonics* **49** 269

[41] de Jong N, Emmer M, van Wamel A and Versluis M 2009 *Med. Biol. Eng. Comput.* **47** 861

[42] Guo X S, Li Q, Zhang Z, Zhang D and Tu J 2013 *J. Acoust. Soc. Am.* **134** 1622

[43] Dayton P A, Morgan K E, Klibanov A L, Brandenburger G E and Ferrara K W 1999 *IEEE Trans. Ultrason. Ferrelec. Freq. Control* **46** 220

[44] Matula T J, Swalwell J, Tu J, Cui W C and Chen W Z 2012 *IEEE Int. Ultrason. Symp.* (IUS) pp. 156–159

[45] Tu J, Guan J F, Qiu Y Y and Matula T J 2009 *J. Acoust. Soc. Am.* **126** 2954

[46] Wu J and Nyborg W L 2008 *Adv. Drug Deliver. Rev.* **60** 1103

[47] Kobayashi N, Yasu T, Yamada S, Kudo N, Kuroki M, Kawakami M, Miyatake K and Saito M 2002 *Ultrasound Med. Biol.* **28** 949

[48] Maruvada S and Hynynen K 2004 *Ultrasound Med. Biol.* **30** 67

[49] Feril L B, Kondo T, Zhao Q L, Ogawa R, Tachibana K, Kudo N, Fujimoto S and Nakamura S 2003 *Ultrasound Med. Biol.* **29** 331

[50] Yu H and Xu L 2014 *J. Control. Release* **174** 151

[51] Miller D L and Thomas R M 1995 *Ultrasound Med. Biol.* **21** 1059

[52] Flynn H G and Church C C 1988 *J. Acoust. Soc. Am.* **84** 985

[53] Newman C and Bettinger T 2007 *Gene Ther.* **14** 465

[54] Chen S Y, Shohet R V, Bekeredjian R, Frenkel P and Grayburn P A 2003 *J. Am. Coll. Cardiol.* **42** 301

[55] Sheyn D, Kimelman-Bleich N, Pelled G, Zilberman Y, Gazit D and Gazit Z 2008 *Gene Ther.* **15** 257

[56] Duvshani-Eshet M, Benny O, Morgenstern A and Machluf M 2007 *Mol. Cancer Ther.* **6** 2371

[57] Duvshani-Eshet M and Machluf M 2007 *Cancer Gene Ther.* **14** 306

[58] Collins C G, Tangney M, Larkin J O, Casey G, Whelan M C, Cashman J, Murphy J, Soden D, Vejda S, Mckenna S, Kiely B, Collins J K, Barrett J, Aarons S and O'Sullivan G C 2006 *Cancer Gene Ther.* **13** 1061

[59] Craig R, Cutrera J, Zhu S, Xia X, Lee Y H and Li S 2008 *Mol. Ther.* **16** 901

[60] Marston P L 1991 *Appl. Opt.* **30** 3479

[61] Bohren C F and Huffman D R 1998 *Absorption and scattering of light by small particles* (GmbH: Wiley-VCH Verlag)

[62] Paul S, Katiyar A, Sarkar K, Chatterjee D, Shi W T and Forsberg F 2010 *J. Acoust. Soc. Am.* **127** 3846

[63] Tsiglifis K and Pelekasis N A 2008 *J. Acoust. Soc. Am.* **123** 4059

[64] Chen W S, Matula T J, Brayman A A and Crum L A 2003 *J. Acoust. Soc. Am.* **113** 643

[65] Li Q, Matula T J, Tu J, Guo X S and Zhang D 2013 *Phys. Med. Biol.* **58** 985

[66] Chang P P, Chen W S, Mourad P D, Poliachik S L and Crum L A 2001 *IEEE Trans. Ultrason. Ferrelec. Freq. Control* **48** 161

[67] Tu J, Matula T J, Brayman A A and Crum L A 2006 *Ultrasound Med. Biol.* **32** 281

[68] Apfel R E and Holland C K 1991 *Ultrasound Med. Biol.* **17** 179

[69] Deng C X, Xu Q H, Apfel R E and Holland C K 1996 *J. Ultrasound Med. Biol.* **22** 939

[70] Deshpande M C and Prausnitz M R 2007 *J. Control. Release* **118** 126

[71] Mitragotri S 2005 *Nat. Rev. Drug Discov.* **4** 255

[72] Tsivgoulis G and Alexandrov A V 2007 *Neurotherapeutics* **4** 420

[73] Miller D L, Pislaru S V and Greenleaf J E 2002 *Somat Cell Mol. Genet.* **27** 115

[74] Qiu Y, Luo Y, Zhang Y, Cui W, Zhang D, Wu J, Zhang J and Tu J 2010 *J. Control. Release* **145** 40

[75] Zhang C B, Cao H L, Li Q, Tu J, Guo X S, Liu Z and Zhang D 2013 *Ultrasound Med. Biol.* **39** 161

[76] Ohl C D and Wolfrum B 2003 *Bba-Gen. Subjects* **1624** 131

[77] Park J, Fan Z Z and Deng C X 2011 *J. Biomech.* **44** 164

[78] Qiu Y Y, Zhang C B, Tu J and Zhang D 2012 *J. Biomech.* **45** 1339

[79] Tran T A, Roger S, Le Guennec J Y, Tranquart F and Bouakaz A 2007 *Ultrasound Med. Biol.* **33** 158